The 6th International Conference on
Structural Health Monitoring of Intelligent Infrastructure
Hong Kong | 9-11 December 2013

DAMAGE CLASSIFICATION USING SUPPORT VECTOR MACHINES IN GUIDED WAVE STRUCTURAL HEALTH MONITORING

Xiang Li [1], Daewon Kim [2] and Yi Zhao [2]
[1] Safety Supervising Department, HNA Aviation Holding, Haikou, Hainan, China
[2] Department of Aerospace Engineering, Embry-Riddle Aeronautical University, Daytona Beach, Florida, USA
Email: daewon.kim@erau.edu

ABSTRACT

A methodology for structural damage classification using a time-frequency representation and Support Vector Machine learning algorithm is investigated. Piezoceramic actuators are utilized to generate guided Lamb wave signals on a set of aluminum beams with different damage features, such as type, location, and extent. The reflected wave signals from damages are sensed by collocated piezoceramic sensors. To get damage information, the sensed damage signals are processed through the short-time Fourier transform that provides both time and frequency information. For damage classification, the spectrograms obtained from finite element analysis are employed to train the machine learning algorithm. The trained algorithm is then used to classify different types and their extents for the tested damage sources. Binary classification is firstly performed for two types of common metallic damages, i.e. crack and corrosion. For the crack damage, multiclass classification is further carried out to evaluate the approximate crack depths.

KEYWORDS

Structural health monitoring, multiclass damage classification, Support Vector Machine, short-time Fourier transform.

INTRODUCTION

In the past decades, rapid developments in the transportation, infrastructure, and manufacturing industries have brought great advantages to humanity. However, catastrophic structural failures, such as building collapses and aircraft incidents, have caused losses of human lives and had significant impacts to the economy. These incidents have emphasized the importance of structural safety and promoted the development of damage detection and identification methods. Among these methods, nondestructive evaluation (NDE) has been widely used in the industries. NDE is a method that examines structural components without affecting object's future usefulness (Shull, 2002). The reliability of NDE can be affected by various factors including inspectors' experiences, working environments, inevitable human errors, etc. To overcome some of these drawbacks of NDE, another damage identification approach called structural health monitoring (SHM) has been developed. SHM is an advanced damage evaluation scheme that consists of multiple transducers, data transmission, computational power, and processing ability. It can provide real time information about damage and may estimate the remaining useful life of structural components. Various SHM methods have been investigated in the past, including the vibration based method, the impedance based method, and the guided Lamb wave based method. The guided Lamb wave, guided wave hereafter, based approach is widely accepted since it is also capable for far-field damage detection (Sun *et al*. 1995). Common SHM methods consist of three general steps, i.e. detection, diagnosis, and prognosis. Damage detection is finding the existence and locations of damage. Damage diagnosis is providing information about damage types and extents. Lastly, damage prognosis is estimating the remained useful life of structural system. There has been considerable research regarding damage detection and diagnosis. Specifically, structural damage classification using various machine learning algorithms has been extensively investigated by many researchers. For instance, a structural health monitoring system has been developed to detect approximate damage locations in beam structures using Support Vector Machines (SVM) and the vibration based method (Liu and Meng 2005). The system was further developed to predict the damage location more accurately using Support Vector Regression. Acoustic emission signals generated by different sources, such as damage growth, have been classified using SVM (Esterline *et al*. 2010). An SHM system has been developed to classify damage signatures in composite structures (Das *et al*. 2007). The system detected the signal responses of surface-mounted piezoelectric transducers and used them to establish a

classifier based on one-class SVM algorithm. A reliable SHM application has been investigated to monitor damages within a pipeline using three classification algorithms including adaptive boosting, SVM, and a method called AdaSVM that combines these two methods (Ying *et al*. 2011). The system was robust enough to resist interferences like changes of internal air pressure in a pipe. The analysis result showed the AdaSVM algorithm achieved the best classification accuracy. A method has been studied to determine the exact location and the area extent of corrosion in an aluminum plate using guided waves generated by a sparse array of ultrasonic transducers (Michaels and Michaels 2007). A classification method has been developed to classify impact-induced damages in composite plates using the finite element analysis and artificial neural networks (Dua *et al*. 2001). A damage classification method that classified crack and corrosion using spectrogram and Adaboost has been investigated (Kim and Philen 2011). The method was able to classify two different damages of crack and corrosion and showed confidence levels of each testing sample. The least square SVM and acoustic signal have been utilized to develop a damage signal classification method (Wang *et al*. 2006). The method exhibited good performance in classifying different types of damage activities over oil transmission pipelines, such as drilling, hammering, and excavating. A method that could correctly diagnose faults in an induction machine has been investigated based on transient current signals (Widodo and Yang 2008). The wavelet transform, SVM, and feature extraction methods were utilized in the research. A motor fault diagnosis method has been developed based on short time Fourier transform and SVM (Banerjee and Das 2012). The method incorporated information collected from multiple sensors to detect and identify the motor faults. A methodology that incorporated SVM and the guided-wave has been developed to classify the extent of growing cracks in lug joints (Coelho *et al*. 2008). In the method, matching pursuit algorithm is utilized to extract feature vectors from raw signals. A method has been developed to detect the abnormal status of a cable-stayed bridge in Zhanjiang, China based upon parameters collected from various sensors attached to the bridge (Vines-Cavanaugh *et al*. 2010). The method utilized an SVM algorithm called SVM20 for status classification and a finite element tool named ANSYS for generating training samples. A damage identification strategy for carbon fiber reinforced polymer composite materials has been developed (Farooq *et al*. 2012). In the method, static strains sensed at predefined locations are measured in different damage scenarios and utilized as features in feature vectors. SVM and artificial neural networks were employed to examine the classification accuracies. A damage detection method has been developed based on the vibration based method and SVM (Xiao and Qu 2012). Different damage states and positions were correctly identified in the method by analyzing vibration signals in different damage scenarios. A damage identification method using SVM and the vibration based method has been investigated (Yang and Liu 2009). Random noises were added into training samples to obtain finite element models for consistency with the real testing sample. Damage location and its extent were able to be predicted by this method. As mentioned, a great amount of research has been conducted on damage detection and classification for various structural components. Many of these researches have utilized various analysis methods to distinguish different types of damages. Some researchers have developed approaches to determine damage locations and others have investigated some methods to monitor the initiation of damages. However, not much attention has been given to damage extent evaluation using the guided wave based SHM method and multiclass SVM classification algorithms. Therefore in this paper, a robust structural damage classification method using multiclass SVM classification is developed to classify multiple classes of structural damages.

TECHNICAL OBJECTIVE AND APPROACHES

The technical objective of this research is to develop a robust damage classification method using time-frequency representation and multiclass SVM classification algorithm to distinguish different types of metallic damages and their severities. In the first step, a binary class damage classification for crack and corrosion damages is developed. Secondly, for the crack damages, multiclass classification using the algorithm is performed to evaluate various crack depths. In order to perform these, various damage scenarios are created by making cracks and corrosion on aluminum beams. Piezoceramic actuators are attached to the aluminum beams to generate guided waves that propagate along the beams. Some portions of the guided waves are reflected by damages on the beams and picked up by piezoceramic sensors. The sensed signals are transformed using short time Fourier transform to generate spectrograms. The spectrograms of various damage signals are used as training samples to train the SVM algorithm. The spectrograms of testing samples are also used to verify the performance and reliability of this method.

DAMAGE CLASSIFICATION USING SUPPORT VECTOR MACHINES

Analysis Setup

As previously mentioned, damage signals for training samples are collected and analyzed in different damage scenarios. However, setting up the experimental environments for all the damage scenarios is both expensive

and time consuming. Instead of performing numerous experiments to get the training samples, a finite element analysis tool, Abaqus®, is employed to simulate various damage models. A crack and a corrosion damages in Abaqus® are illustrated in Figure 1. In the figure, two 1 cm by 1 cm thin piezoceramic, or PZT, actuators are attached at the center of a thin 2 m aluminum beam. The positive poles of the PZTs face the opposite direction to each other. A crack is represented as a thin notch and located at a distance "d" from the actuators. The width of a crack is 1 mm. The depth "t" of a crack varies from 1/8 to 6/8 of the thickness of the aluminum beam (3 mm). In Figure 1 (b), corrosion is also placed at a distance of "d" from the actuators. It can be observed that its cross section is shaped as a trapezoidal channel with a width of 3 cm. This is done so since a crack is generally initiated narrow and sharp in one direction but corrosion has a large affected area in all directions. Other dimensions and setups for the corrosion damage are similar to the crack damage.

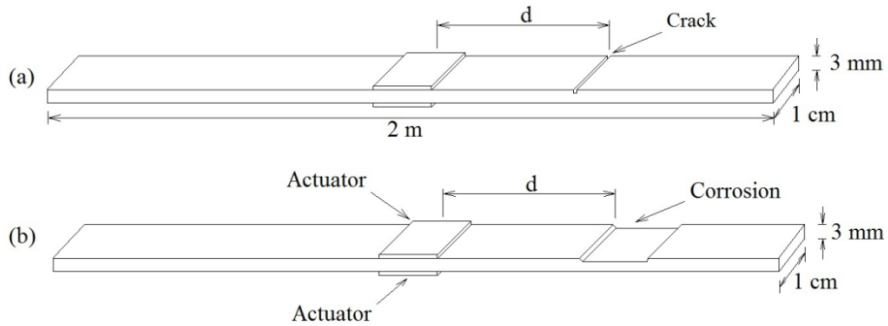

Figure 1. Damage scenarios in Abaqus® for (a) crack damage and (b) corrosion damage

A 2.5 cycle, Hanning windowed, tone-burst signal is generated by two PZT actuators which excite only A_0 mode. The sensed signal, shown in Figure 2(a), is obtained at a location close to the PZT actuator on the upper surface of the beam. It contains both the actuated signal (solid rectangle) and the reflected signal (dashed rectangle). The center frequency of the excited signal is 50 kHz and, since the beam thickness is 3 mm, the A_0 and S_0 group velocities are obtained around at 2.1 km/s and 5.4 km/s, respectively, as shown in Figure 2(b).

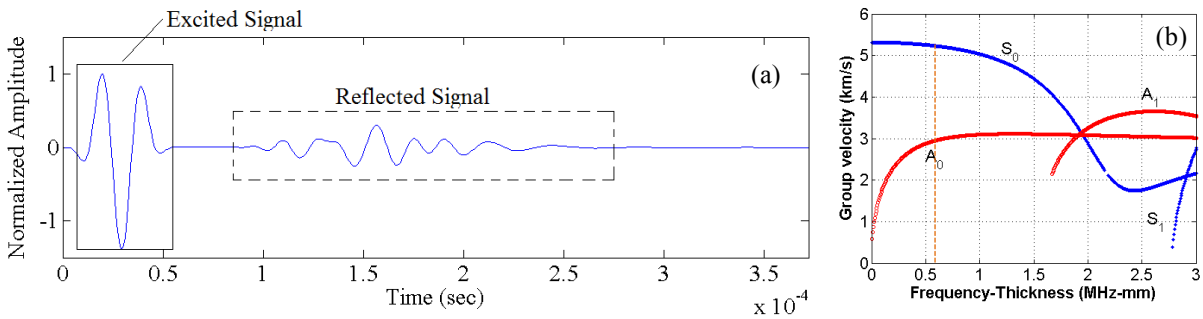

Figure 2. (a) Sensed corrosion (d=15 cm, 3/8th of beam thickness) damage signal containing the excited and the reflected signals and (b) group velocity dispersion curves for aluminum alloy

Damage features are included only in the reflected signal, inside of the dashed rectangle. Therefore in order to analyze the damage signals, the excited signal should be eliminated from the whole sensed signal. The reflected crack damage signal after the removal is therefore shown in Figure 3(a), as well as the spectrogram of the reflected signal using short time Fourier transform, in Figure 3(b). Note that the sensed signal contains both faster S_0 mode and slower A_0 mode although only the A_0 mode is excited. This is due to a dual-mode guided wave reflection per a single-mode wave at the crack boundary. The spectrogram clearly shows these two modes. Although the center frequency of the excited signal is 50 kHz, the damage signal has frequency boundaries of ±30 kHz, i.e. 20 kHz to 80 kHz with the center frequency at 50 kHz. In this spectrogram, different levels of spectrogram intensity represent different levels of energy density. The reflected signal has a large peak at S_0 mode compare to A_0 mode and this peak, the highest energy density, is shown as a true red color in the normalized spectrogram.

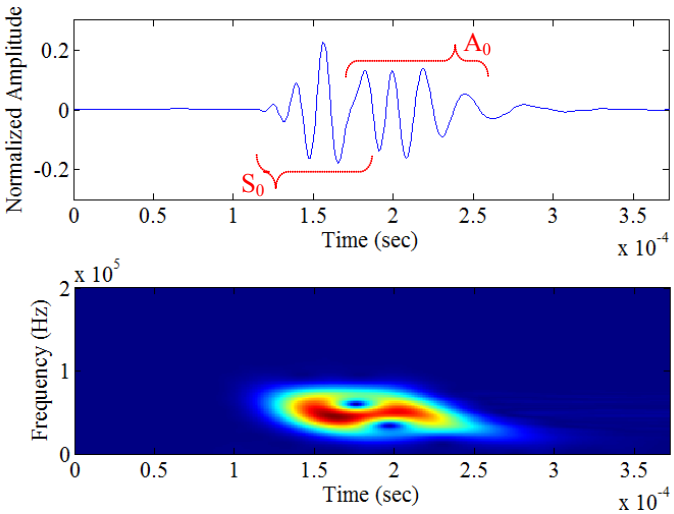

Figure 3. Reflected damage signal with two modes (top) and its spectrogram using short time Fourier transform (bottom)

Spectrogram Analysis

As previously mentioned, much damage information can be found from the spectrograms, including wave modes, distance to damage, frequency, and even damage size. It is therefore chosen to distinguish two common types of metallic damage, i.e. crack and corrosion. Figure 4 shows the spectrograms of four different crack signals in part (a) and corrosion signals in part (b). For this binary damage classification, the energy density of the spectrogram is normalized since superficial damages, such as 1/8th or 2/8th of the plate thickness, produce weak signals. By normalizing them, the energy intensity of the spectrogram for all the crack and corrosion signals looks similar as shown in the figure. However, their overall shapes for crack and corrosion damages seem quite different by comparing plots in part (a) and (b). Different spectrograms have different energy density distributions, which are represented by different color distributions in the spectrogram. Therefore, to distinguish different types of damages, it is desired to extract the color information from the spectrogram.

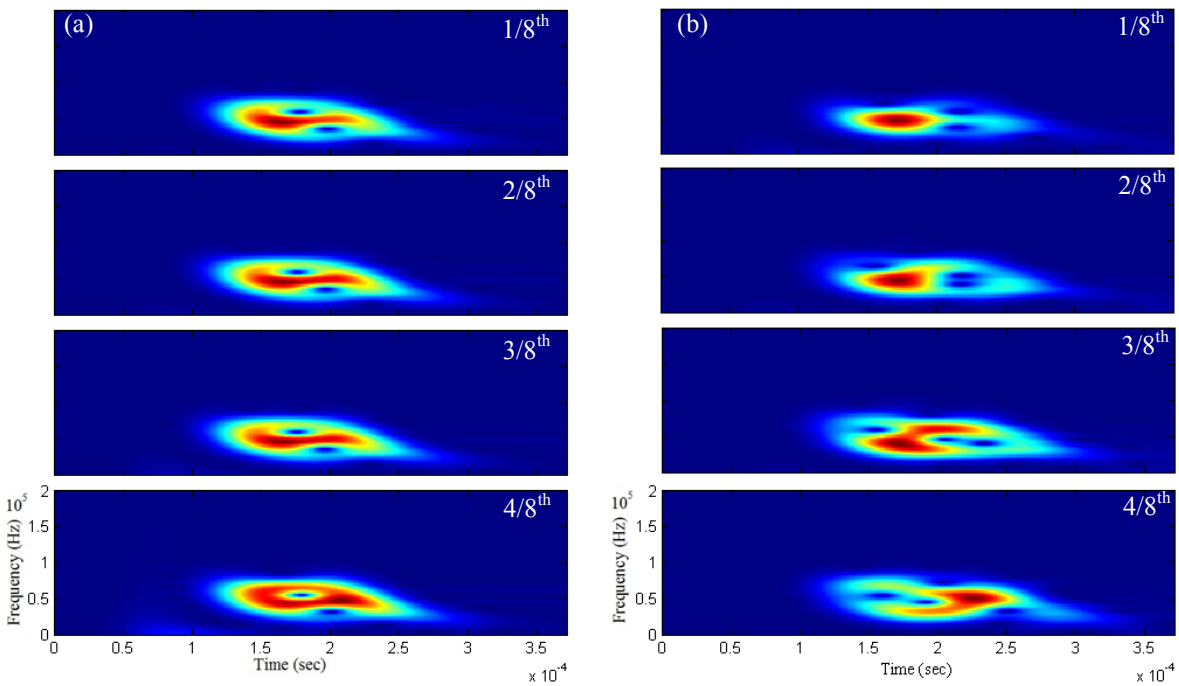

Figure 4. Normalized spectrograms of various damage signals for (a) cracks and (b) corrosion at d=20 cm, both for 1/8th, 2/8th, 3/8th, 4/8th of beam thickness (top to bottom)

The color information of each pixel of the spectrogram is extracted as shown in the magnified image of Figure 5. In this paper, a spectrogram is saved as a 24 bit true color image. In the spectrogram image, each of the red, green, and blue (RGB) color channels has 256 (8-bit) levels of color depth. Different colors can be described by different combinations of RGB color channel depths. For instance, the "white" color is represented by Red-255, Green-255, and Blue-255. On the other hand, the "black" color is represented by Red-0, Green-0, and Blue-0. In Figure 5 (b), the color channel depth information of the "blue" pixel marked by the white square is extracted using computer tools as: Red-0, Green-0, and Blue-236.

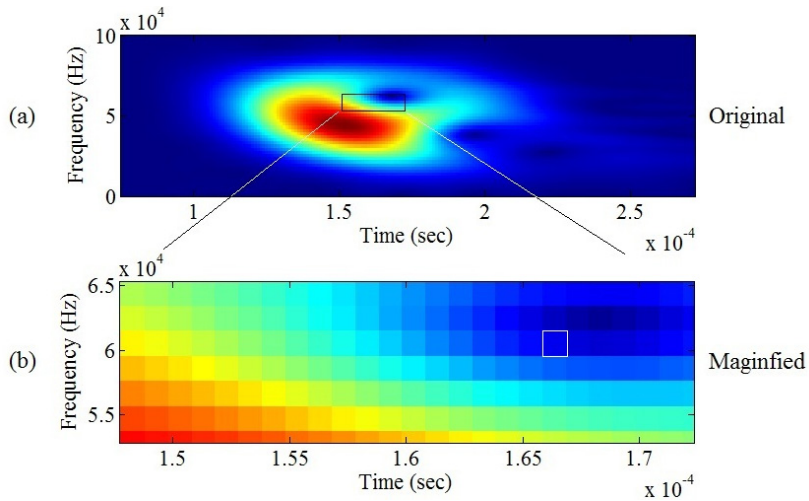

Figure 5. A pixel in a magnified portion of a spectrogram and its RGB color depths

Feature Vectors in Support Vector Machines

The previous process can be used to extract color depth information for all pixels in a spectrogram. Different spectrograms have different distributions of color channel depth information. Therefore, the distributions of RGB color depth in pixels can be used as "features" to describe a spectrogram. Furthermore, these color depths of all pixels in a spectrogram can be reorganized to generate the feature vectors for training and testing of an SVM algorithm. Although these color depths would make sufficient feature vectors, in order to make the algorithm more robust and to improve classification accuracy, frequency information of each pixel is also added onto the color depth of each pixel, as shown in Figure 6. First three cells, RGB, represent the color depth and the fourth one, f, is the additional frequency information. For instance, the pixel in the white square in Figure 5(b) represents a frequency around 6.1×10^4 Hz. Then, the feature vector of this cell would be, by combining it with the color depths, [0 0 236 6.1×10^4].

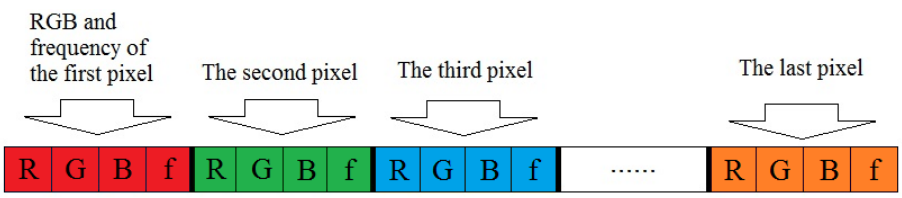

Figure 6. Arrangement of a feature vector of training or testing sample

As shown in Figure 6, color depths and frequencies for all pixels in a spectrogram are chained together in an order to generate a lengthy feature vector for SVM. The RGB color depth information of the first pixel in a spectrogram (1st row and 1st column) is placed first and the second one (1st low and 2nd column) is followed immediately. This process is repeated upon all other pixels in the spectrogram until the RGB color depth and frequency for the last pixel (last low and last column) are saved in the last 4 elements in the feature vector. The length of a feature vector is related to the size of a spectrogram image. For instance, for the spectrogram with 500 column pixels and 250 row pixels, the number of elements of the feature vector is 500,000. Feature vectors for the damage signals for other damage scenarios can be obtained using the same approach.

RESULTS AND DISCUSSIONS

Binary Classification

For the binary classification of crack and corrosion, 80 damage samples (40 cracks and 40 corrosions) have been simulated using Abaqus®. Damage signals obtained in these damage scenarios are used to generate training samples for damage classification. The distances between the damages and the PZT actuators of the samples vary from 10 cm to 22 cm. The depths of the damages also vary among $1/8^{th}$, $2/8^{th}$, $3/8^{th}$, $4/8^{th}$ and $6/8^{th}$ of the beam thickness. All the damage samples are divided into two classes per the damage types (crack and corrosion). Among these, 64 samples are used as the training samples to train a binary SVM classifier. 16 samples are used as testing samples to examine the accuracy of the binary classifier. The training and testing samples are described in Table 1.

Table 1. Training and testing samples for the binary classification
re

	Damage Type	Distance between the damage and the PZT	Damage Depth
64 Training Samples	Crack	10 cm, 13 cm, 15 cm, 16 cm, 18 cm, 19 cm, 20 cm, 22 cm	1/8, 2/8, 4/8, and 6/8 of the beam thickness
	Corrosion	10 cm, 13 cm, 15 cm, 16 cm, 18 cm, 19 cm, 20 cm, 22 cm	1/8, 2/8, 4/8, and 6/8 of the beam thickness
16 Testing Samples	Crack	10 cm, 13 cm, 15 cm, 16 cm, 18 cm, 19 cm, 20 cm, 22 cm	3/8 of the beam thickness
	Corrosion	10 cm, 13 cm, 15 cm, 16 cm, 18 cm, 19 cm, 20 cm, 22 cm	3/8 of the beam thickness

In the training process of the binary SVM classification, all the 64 training samples were utilized to train a two-class classifier. A high cross validation accuracy of 89.06% was obtained in the training process. In the testing process, each of the 16 testing samples was predicted by the classifier. The testing sample's predicted damage type was compared with its original damage type to examine if the classification was correct. All the 16 testing samples were correctly classified by the binary classifier. Therefore, the binary classifier exhibited high classification accuracy for the binary classification of crack and corrosion damages.

Multiclass Classification

The second objective of this paper is to develop a multiclass classification to evaluate the crack extent. As previously mentioned, the energy density in a spectrogram is normalized in the binary classification for crack and corrosion damages. For the multiclass classification, however, the energy density of each crack signal is not normalized. This is due to the fact that the reflected wave by a deep crack yields relatively large energy whereas a superficial crack produces relatively small energy. The actual energy distribution of the reflected wave is crucial for the multiclass classification. Figure 7 shows the spectrograms of four different crack signals for the multiclass classification. The depths of cracks vary from $1/8^{th}$ to $4/8^{th}$ of the beam thickness. It can be observed that the colors in the spectrogram become more intense as the crack depth increases since the energy density of the reflected signal becomes stronger as the crack depth increases.

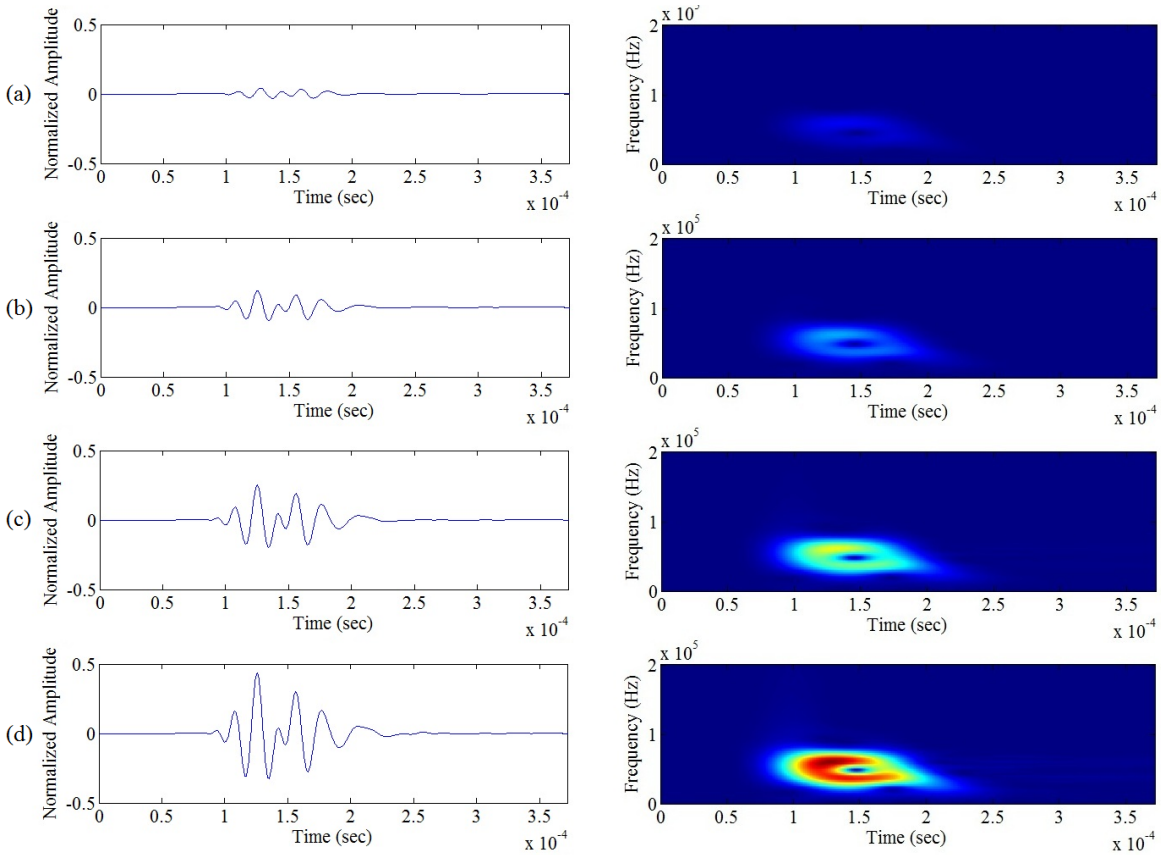

Figure 7. Spectrograms of different crack signals (d=15 cm) for the multiple-class classification (a) 1/8th, (b) 2/8th, (c) 3/8th, and (d) 4/8th of beam thickness

As shown in the figure, for the multiclass classification, all crack samples are divided into four classes, i.e. starting from 1/8th and increasing every 1/8th to 4/8th of the beam thickness. Total of 60 crack samples are used as the training samples and 12 crack samples are used as the testing samples. The damage locations of all the 72 samples vary from 10 cm to 27 cm with an interval of 1 cm. The cross validation accuracy of the 4-class classifier for the training samples is 70% and, in the testing samples, 9 out of the 12 testing samples are correctly classified.

It turns out that the performance of the multiclass classifier is not as good as the binary classifier. To further analyze the results, 15 training samples with 1/8 of the beam thickness are taken out from the 60 training samples and the remained training samples with 2/8, 4/8, and 6/8 of the beam thickness are used to train a three-class classifier. The cross validation of this three-class classifier is found to be 91.11%, about 20% higher than using four classes. With the three-classifier, all 9 testing samples are correctly classified. Similarly, more combinations of the training samples are also tested to observe the cross validation accuracy and their results are shown in Figure 8.

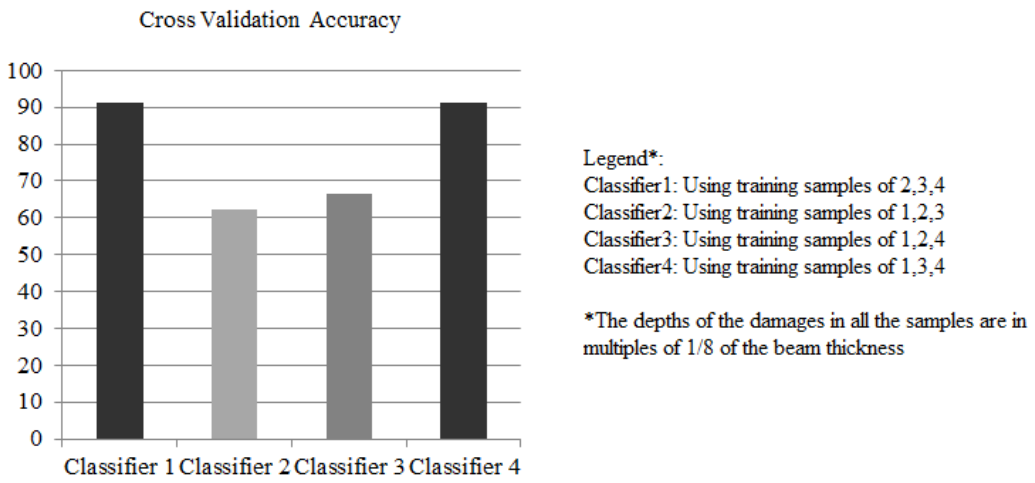

Figure 8. The cross validation accuracies of different three-class classifiers

In Figure 8, it turns out that the cross validation accuracies are generally low if the training samples contain samples from both Class 1 and Class 2. However, a three-class classifier can provide good cross validation accuracy, as long as the samples from Class 1 and Class 2 are not used for training simultaneously. This is mainly due to that the spectrograms of Class 1and Class 2 are quite similar, as shown in Figures 7(a) and 7(b). The similarity in the spectrograms between Class 1 and Class 2 affects the training and testing processes for SVM classification.

To overcome this drawback, the crack signals for $1/8^{th}$ of the beam thickness are removed from the training samples and the new cracks of $6/8^{th}$ of beam thickness are considered. Hence, the cracks with $2/8^{th}$, $4/8^{th}$, and $6/8^{th}$ of the beam thicknesses are used as training samples to conduct another three-class damage classification. For this analysis, 45 cracks samples are used as the training samples and 9 other cracks samples are used as testing samples. The damage locations of testing samples vary among 13 cm, 14 cm, and 24 cm. The depths of testing samples vary among $2/8^{th}$, $4/8^{th}$, and $6/8^{th}$ of the beam thickness. Based on these samples and a three-class classifier of 45 samples, the cross validation accuracy is found to be 88.89% and all the testing samples are correctly classified using this classifier. Therefore, it can be concluded that multiclass classification may not yield good performance results if the training samples contain more than one class of superficial damages, such as crack depths of $1/8^{th}$ or $2/8^{th}$ of the beam thickness. However, it can exhibits good performance if the training samples contain only one class of superficial damage.

CONCLUSIONS

In this paper, a robust structural damage classification method using spectrograms and Support Vector Machine is developed. This method results in high classification accuracy for the binary classification of crack and corrosion damages. Multiclass classification is also examined for cracks with different crack depths. The results show that the performance of multiclass classification is limited if the training and testing damage samples contain more than one class of superficial damages. However, the method yields high classification accuracy as long as the training and testing samples contain minimum, only one in this case, number of superficial damage. For future work, it is recommended to develop a more reliable classifier that can classify different damage classes containing more than one class of superficial damage. In addition, a damage evaluation method using SVM regression can be investigated to evaluate the actual depths of cracks.

REFERENCES

Shull, P.J. (2002). *Nondestructive Evaluation Theory, Techniques, and Applications*, New York: Marcel Dekker, Inc.

Sun, F.P., Chaudhry, Z., Liang, C. and Rogers, C.A. (1995). "Truss structure integrity identification using PZT sensor-actuator", *Journal of Intelligent Material Systems and Structures*, vol. 6, 134-139.

Liu, L. and Meng, G. (2005). "Localization of damage in beam-like structures by using Support Vector Machine", *International Conference on Neural Networks and Brain*, v.2, 919-924.

Esterline, A., Krishnamurthy, K., Sundaresan, M., Alam, T., Rajendra, D. and Wrigft, W. (2010). "Classifying acoustic emission data in structural health monitoring using Support Vector Machines", *AIAA Infotech at Aerospace*.

Das, Santanu, Ashok N. Srivastava, and Aditi Chattopadhyay (2007). "Classification of damage signatures in composite plates using one-class SVMs", *IEEE Aerospace Conference Proceedings*.

Ying, Y., Harley, J., Garrett Jr., J.H., Jin, Y., Oppenheim, I.J., Shi, J. and Soibelman, L. (2011). "Applications of machine learning in pipeline monitoring", *Congress on Computing in Civil Engineering*, 242-249.

Michaels, T.E., and Michaels, J.E. (2007). "Monitoring and characterizing corrosion in aluminum using Lamb waves and attached sensors", *Proceedings of SPIE-The International Society for Optical Engineering*, v 6532.

Dua, R., Watkins, S.E., Wunsch, D.C., Chandrashekhara, K. and Akhavan, F. (2001). "Detection and classification of impact-induced damage in composite plates using neural networks", *Proceedings of the International Joint Conference on Neural Networks*, v 1, pp. 681-686.

Kim, D. and Philen, M. (2011). "Damage classification using adaboost machine learning for structural health monitoring", *Proceedings of SPIE - The International Society for Optical Engineering*, v 7981.

Wang, Q., Yuan, C. and Zhu, J. (2006). "Buried pipeline third-party damage signals classification based on LS-SVM", *Proceedings of the World Congress on Intelligent Control and Automation*, v 1, 5032-5036.

Widodo, A., and Yang, B.S. (2008). "Wavelet Support Vector Machine for induction machine fault diagnosis based on transient current signal", *Expert Systems with Applications*, v 35, 307-316.

Banerjee, T.P. and Das, S. (2012). "Multi-sensor data fusion using Support Vector Machine for motor fault detection", *Information Sciences*, v 217, 96-107.

Coelho, C.K., Das, S. and Chattopadhyay, A. (2008). "Binary tree SVM based framework for mining fatigue induced damage attributes in complex lug joints", *Proceedings of SPIE - The International Society for Optical Engineering*, v 6926.

Vines-Cavanaugh, D., Cao, Y., and Wang, M.L. (2010). "Support vector machine for abnormality detection on a cable-stayed bridge", *Proceedings of SPIE - The International Society for Optical Engineering*, v 7647.

Farooq, M., Zheng, H., Nagabhushana, A., Roy. S., Burkett, S., Barkey, M., Kotru, S., and Sazonov E. (2012). "Damage detection and identification in smart structures using SVM and ANN", *Proceedings of SPIE 8346, Smart Sensor Phenomena*, Technology, Networks, and Systems Integration.

Xiao, L., and Qu, W. (2012). "Nonlinear structural damage detection using Support Vector Machines", *Proceedings of SPIE - The International Society for Optical Engineering*, v 8348.

Yang, Y., and Liu, T.Y. (2009). "Application of Support Vector Machine in structure damage identification", *Proceedings - International Conference on Information Engineering and Computer Science*.